eISSN 2005-5447
International Journal of Stem Cells Vol. 17, No. 1, 2024 https://doi.org/10.15283/ijsc23101

ORIGINAL ARTICLE

Nervonic Acid Inhibits Replicative Senescence of Human Wharton's Jelly-Derived Mesenchymal Stem Cells

Sun Jeong Kim[1,2,*], Soojin Kwon[1,2,*], Soobeen Chung[1,2,*], Eun Joo Lee[1,2], Sang Eon Park[1,2], Suk-Joo Choi[3], Soo-Young Oh[3], Gyu Ha Ryu[4,5], Hong Bae Jeon[1], Jong Wook Chang[1,2,6]

[1]*Cell and Gene Therapy Institute, ENCell Co. Ltd., Seoul, Korea*
[2]*Cell and Gene Therapy Institute, Samsung Medical Center, Seoul, Korea*
[3]*Department of Obstetrics and Gynecology, Samsung Medical Center, Seoul, Korea*
[4]*Department of Medical Device Management and Research, SAIHST, Sungkyunkwan University, Seoul, Korea*
[5]*The Office of R&D Strategy & Planning, Samsung Medical Center, Seoul, Korea*
[6]*Department of Health Sciences and Technology, SAIHST, Sungkyunkwan University, Seoul, Korea*

Cellular senescence causes cell cycle arrest and promotes permanent cessation of proliferation. Since the senescence of mesenchymal stem cells (MSCs) reduces proliferation and multipotency and increases immunogenicity, aged MSCs are not suitable for cell therapy. Therefore, it is important to inhibit cellular senescence in MSCs. It has recently been reported that metabolites can control aging diseases. Therefore, we aimed to identify novel metabolites that regulate the replicative senescence in MSCs. Using a fecal metabolites library, we identified nervonic acid (NA) as a candidate metabolite for replicative senescence regulation. In replicative senescent MSCs, NA reduced senescence-associated β-galactosidase positive cells, the expression of senescence-related genes, as well as increased stemness and adipogenesis. Moreover, in non-senescent MSCs, NA treatment delayed senescence caused by sequential subculture and promoted proliferation. We confirmed, for the first time, that NA delayed and inhibited cellular senescence. Considering optimal concentration, duration, and timing of drug treatment, NA is a novel potential metabolite that can be used in the development of technologies that regulate cellular senescence.

Keywords: Nervonic acid, Replicative senescence, Metabolites, Mesenchymal stem cells

Introduction

Cellular senescence is a state of permanent proliferative interruption caused by cell cycle arrest. It is caused by various factors such as repetitive cell division, DNA damage, the activation of oncogene, oxidative stress, mitochondrial dysfunction, and secretion of paracrine factors Replicative senescence, caused by telomere shortening, reduces proliferation and modifies the expression of growth-regulatory genes. Cellular senescence can be identified by the expression of cyclin-dependent kinase (CDK) inhibitors and senescence-associated secretory phenotype (SASP), cell size measurement, and lysosomal content (1).

Mesenchymal stem cells (MSCs) derived from various adult cells such as bone marrow, cord blood, placenta, and fat are multipotent and have low immunogenicity (2).

Received: June 28, 2023, Revised: August 1, 2023,
Accepted: August 1, 2023, Published online: October 12, 2023
Correspondence to **Jong Wook Chang**
Department of Health Sciences and Technology, SAIHST, Sungkyunkwan University, 115 Irwon-ro, Gangnam-gu, Seoul 06355, Korea
E-mail: jongwook.chang@samsung.com
Co-Correspondence to **Hong Bae Jeon**
Cell and Gene Therapy Institute, ENCell Co. Ltd., 701 Yeongdong-daero, Gangnam-gu, Seoul 06072, Korea
E-mail: jhb@encellinc.com
*These authors contributed equally to this work.

Therefore, MSCs are extensively used in cell therapy. However, ensuring an adequate supply of cells is necessary to commercialize cell therapy using MSCs, as MSCs rapidly reduce cell division by senescence mechanisms during *in vitro* culture. With age, MSCs experience reduced stemness, proliferation and differentiation (3). They undergo morphological changes, becoming enlarged and flattened, and secrete SASP factors. These SASP factors, secreted by aging cells, affect the aging of surrounding cells (4). In addition, senescent MSCs diminish mobility, paracrine effects, and immunomodulatory function (5). This negatively impacts the use of MSCs in cell therapy; therefore, the discovery of senescence regulators is important to develop technologies that can delay or reverse the replicative senescence of MSCs.

The gut microbiome synthesizes a variety of metabolites with powerful anti-inflammatory and antioxidant properties. Increased oxidative stress induces cellular senescence, and microbiota metabolites can diminish cellular senescence by reducing the stress response (6). Alteration in intestinal microbiota composition, in aged mice, causes inflammation in brain and retina and controlling the gut microbial composition prevents age-associated disease (7). In this study, we aimed to identify new senescence control factors that inhibit replicative senescence of MSCs, using fecal metabolites library. The fecal metabolite, nervonic acid (NA), was selected as the potential candidate.

NA (C24 : 1, cis-15-tetracosenoic acid) is a long-chain fatty acids, mainly found in brain sphingolipids, associated with the growth and maintenance of nerve tissue. In addition, it is involved in myelin membrane creation, brain aging inhibition, and lipid metabolism regulation (8, 9). NA accumulates in the human brain during early development, positively influences neonatal neural development (10), and is used in the prevention and treatment of neurological disorders (11). To date, the effects of NA on MSC senescence or function remain unknown. In this study, we evaluated that the effect of NA treatment on senescent cells.

Materials and Methods

MSC culture

Wharton's jelly-derived mesenchymal stem cells (WJ-MSCs), adipose tissue-derived mesenchymal stem cells (AD-MSCs), placenta-derived mesenchymal stem cells (PL-MSCs), and umbilical cord blood-derived mesenchymal stem cells (UCB-MSCs) were isolated from umbilical cord, adipose tissue, placenta, and umbilical cord blood, respectively, as previously described (12-15). Human bone marrow-derived mesenchymal stem cells (BM-MSCs) were purchased from Cambrex (#PT-2501; Lonza). Replicative senescence was induced by sequential culture in MEM-alpha (Minimum Essential Medium; Gibco) with 10% FBS (Fetal Bovine Serum; Gibco) and 50 μg/ml Gentamicin (Gibco) at 37℃ and 5% CO_2.

Metabolite screening

Metabolites were screened using a fecal metabolites library (MetaSci). Four-hundred and eighty-five metabolites were identified. WJ-MSCs were seeded on a 384-well plate and cultured for 24 hours at 37℃ and 5% CO_2. Next, the cultured cells were treated with the identified metabolites (20 μM) and incubated for 72 hours at 37℃ and 5% CO_2. Subsequently, cytotoxicity was measured using high throughput screening. Thirteen candidate metabolites were identified and were used in subsequent analysis. WJ-MSCs were seeded in a 96-well plate at 1,000 cells/well and cultured for 24 hours at 37℃ and 5% CO_2. Next, the cultured cells were treated with the candidate metabolites at different concentrations ranging from 20 to 400 μM and incubated for 72 hours at 37℃ and 5% CO_2. Cell viability was measured using the Cell Counting Kit-8 (CCK-8; Dojindo), according to the manufacturer's instructions. NA (Sigma-Aldrich) was selected through various screening methods. WJ-MSCs were treated with NA at several concentrations ranging between 140 and 260 μM and incubated for 72 hours at 37℃ and 5% CO_2. NA was dissolved in dimethyl sulfoxide (DMSO), and all controls were treated with equal amounts of DMSO. Optical density was measured at 450 nm using a microplate reader (Multiskan SkyHigh; Thermo Fisher Scientific Inc.).

Senescence associated β-galactosidase staining

Cellular senescence was confirmed using a Senescence *B*-Galactosidase Staining Kit (Cell Signaling Technology). After seeding WJ-MSCs at 50,000 cells/well in 6-well plate, the WJ-MSCs were treated with NA for 3 days. The NA-treated WJ-MSCs were fixed with 4% PFA, stained with senescence associated β-galactosidase (SA-β-gal) staining solution and incubated for 24 hours at 37℃. The stained cells were observed under a microscope (Olympus CKX21; Olympus) and analyzed with ImageJ (National Institutes of Health).

Quantitative reverse transcript polymerase chain reaction

Total RNA was isolated from WJ-MSCs using Trizol (Invitrogen) and cDNA was synthesized using Superscript IV RT (Invitrogen), according to the manufacturer's instruc-

tions. Quantitative reverse transcript polymerase chain reaction (qRT-PCR) was performed on QuantStudio 6 Flex Real-Time PCR System (Thermo Fisher Scientific Inc.) using 2x Power SYBR Green Master Mix (Applied Biosystems). Primers were purchased from Bioneer Corporation and the primer sequences were as follow: *p16* Forward 5'-CCCAACGCACCGAATAGTTA-3', Reverse 5'-ACCAGC GTGTCCAGGAAG-3', *p21* Forward 5'-AGGTGGACCTG GAGACTCTCAG-3', Reverse 5'- TCCTCTTGGAGAAGA TCAGCCG-3', *MMP3* Forward 5'- GACTCCACTCACA TTCTCC-3', Reverse 5'- AAGTCTCCATGTTCTCTAACTG-3', *IGFBP5* Forward 5'-GAGCAAGTCAAGATCGAGAG-3', Reverse 5'-CTTCTTCACTGCTTCAGCC-3', *IGFBP7* Forward 5'-CAAAGGACAGAACTCCTGC-3', Reverse 5'-TAGAGGAGATACCAGCACC-3', *GAPDH* Forward 5'-GAAGGTGAAGGTCGGAGT-3', Reverse 5'- TGGCAACA ATATCCACTTTACCA-3'. Relative gene expression was calculated using the $2^{-\Delta\Delta Ct}$ method. Gene expression was normalized to that of *GAPDH*.

Western blot analysis

Cells were lysed using RIPA buffer (BIOSESANG) with the Protease Inhibitor Cocktail (GenDEPOT) and EDTA (GenDEPOT). The Bradford assay (Bio-Rad protein assay reagent; Bio-Rad) was used to quantify protein concentration. Equivalent amounts of protein were separated using SDS-PAGE and transferred to polyvinylidene difluoride membranes (Bio-Rad). The membranes were blocked with 5% skim milk for 1 hour at room temperature and incubated for 24 hours at 4℃ with the following primary antibodies: anti-p16 (1 : 1,000; Cell Signaling Technology), anti-p21 (1 : 1,000; Cell Signaling Technology), anti-β-actin (1 : 5,000; Santa Cruz). Next, the membranes were incubated with HRP-conjugated anti-rabbit or anti-mouse antibodies (AbClon) for 1 hour at room temperature. Signals were detected using the Amersham Imager 600 (GE Healthcare), and band intensities were quantified using ImageJ. β-Actin was used as the loading control. Expression was normalized to that of β-actin.

Stemness analysis

To verify WJ-MSCs stemness, the expression of MSC and hematopoietic markers were confirmed using flow cytometry, as per the MSC criteria of the International Society for Cell Therapy (16). Cells were incubated with the following antibodies: cluster of differentiation 44 (CD44), CD73, CD90, CD105, CD166, CD14, CD19, CD34, CD45, HLA-DR, or isotype control antibodies (BD Biosciences) for 20 minutes at room temperature in the dark. At least 10,000 events were acquired using the BD FACSVerse (Becton Dickinson), and data analysis was performed using FACSuite software (Becton Dickinson).

Adipogenic differentiation assay

WJ-MSCs were seeded at 1×10^5 cells/well in a 6-well plate. After changing the complete culture media, WJ-MSCs were cultured to 100% growth. The culture media was changed as indicated in the Stempro Adipocyte Differentiation Kit (Gibco), and the WJ-MSCs were cultured for 21 days in differentiation media with or without NA. Differentiated cells were fixed with 4% PFA for 10 minutes at room temperature. Oil Red O solution (Sigma-Aldrich), dissolved in isopropyl alcohol (Sigma-Aldrich), was added to the fixed cells. Oil Red O optical density was measured at 510 nm using Multiskan SkyHigh.

Osteogenic differentiation assay

WJ-MSCs were seeded at 5×10^4 cells/well in a 6-well plate. The culture media was changed as indicated by the Stempro Osteocyte Differentiation Kit (Gibco) and WJ-MSCs were cultured for 23 days in differentiation media with or without NA. The cultured cells were fixed with 4% PFA, and the differentiated cells were using Alizarin Red S Staining Quantification Assay Kit (ScienCell), according to the manufacturer's instructions. Alizarin Red S was dissolved in 10% acetic acid, and optical density was measured at 405 nm using Multiskan SkyHigh.

Antibody array analysis

The Human L507 array was performed by Ebiogen Inc.. The culture medium was concentrated 10 times using Vivaspin 15R (Sartorius). The sample concentration was measured using BCA Protein Assay Kit (Pierce) and Multiskan FC (Thermo Fisher Scientific Inc.). Slide scanning was performed using the GenePix 4100A Scanner (Axon Instruments), and scan images were quantified with GenePix Software (Axon Instruments). Data mining and graphic visualization were performed using ExDEGA (Ebiogen Inc.).

Single-cell RNA sequencing

Single-cell RNA sequencing was conducted by Ebiogen Inc.. Single-cell RNA-sequencing libraries were prepared using the Chromium Next GEM Single Cell 3' Reagent Kit v3.1 (10X Genomics), according to the manufacturer's instructions. The cells were diluted into the Chromium Next GEM Chip G to yield a recovery of 6,000 single-cell. Following library preparation, the libraries were sequenced in multiplex on the Novaseq 6000 sequencer (Illumina) to produce, on average, a minimum of 45,000 reads per single cell. Sequencing reads were processed with the Cell Ranger

version 3.0.1 (10X Genomics) using the Human reference transcriptome GRch38 from Ensemble. Data clustering and visualization were performed using MultiExperiment Viewer, Loupe browser, and Win Seurat (Ebiogen Inc.).

Statistical analysis

All data are represented as means±SEM. GraphPad PRISM (GraphPad software Inc.) was used for analysis. Comparisons between two groups were conducted using a two-tailed Student's t-test, and comparisons between more than two groups were conducted using one-way ANOVA analysis with Tukey's multiple-comparison post hoc test. $p<0.05$ was considered statistically significant. All experiments were performed in triplicate.

Results

Verification of replicative senescence in WJ-MSCs

WJ-MSC replicative senescence was induced by sequential culturing and the level of senescence was confirmed through SA-β-gal staining. The proportion of β-gal positive cells increased negligibly by less than 5% until passage 15 but increased to 42.4% at passage 18 (Fig. 1A).

To determine the induction of replicative senescence, the expression of senescence markers was confirmed using western blotting. The expression of p16 and p21 at passage 18 was significantly higher than that at passage 5. p16 significantly increased at passage 18. p21 significantly increased at passage 9, and the expression level was retained thereafter (Fig. 1B). Therefore, MSCs at passage 18 were defined as replicative senescent MSCs (RS-MSCs) and MSCs at passage 5 as non-senescent MSCs (NS-MSCs).

NA inhibits the replicative senescence in WJ-MSCs

NS-MSCs and RS-MSCs were treated with 485 candidate metabolites and we determined the level of senescence reduction. Compared to NS-MSCs, RS-MSC viability was reduced by 13 metabolites (Supplementary Fig. S1). Among these, NA, which only affected the survival of RS-MSC, was selected for further analysis. To determine the optimal NA concentration that reduces only the survival of RS-MSCs as much as possible, WJ-MSCs were treated with varying concentrations of NA for 3 days. Then, the CCK-8 assay, SA-β-gal staining and cell size measurement were performed to confirm the inhibition of senescence by NA (Fig. 2A). NA did not decrease NS-MSC cell viability, but decreased RS-MSCs cell viability. RS-MSC viability was most significantly reduced by 160 μM NA and was therefore used in subsequent experiments (Fig. 2B).

NS-MSCs and NA-treated NS-MSCs were stained with β-gal in 3.26% and 2.32% of the total cells, respectively, while RS-MSCs and NA-treated RS-MSCs were stained with β-gal in 46.40% and 19.21%, respectively (Fig. 2C). NA treatment significantly reduced senescence only in the RS-MSCs. In addition, cell size, a parameter of senescence, was measured to confirm the reduction of senescent cells by NA. The surface area of RS-MSCs was 3.17-fold larger than that of NS-MSCs. On the other hands, the surface area of NA-treated RS-MSCs was 0.43-fold smaller than that of RS-MSCs (Fig. 2D). Therefore, NA was confirmed to be an effective inhibitor of WJ-MSC senescence.

In addition, SA-β-gal staining was performed to identi-

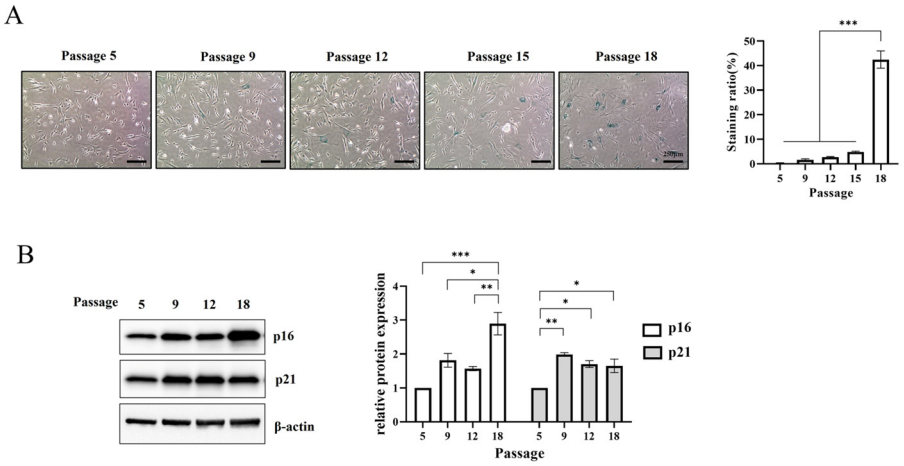

Fig. 1. Induction of replicative senescence in Wharton's jelly-derived mesenchymal stem cells (WJ-MSCs). (A) SA-β-galactosidase staining was performed during sequential subculture. The staining ratio was expressed as the number of stained cells to the total number of cells. Scale bar=250 μm. (B) The protein expression of p16 and p21, according to the passage, was examined by western blot. Data are presented as mean±SEM. The significance of the differences was assessed by one-way ANOVA (*$p<0.05$, **$p<0.01$, ***$p<0.001$).

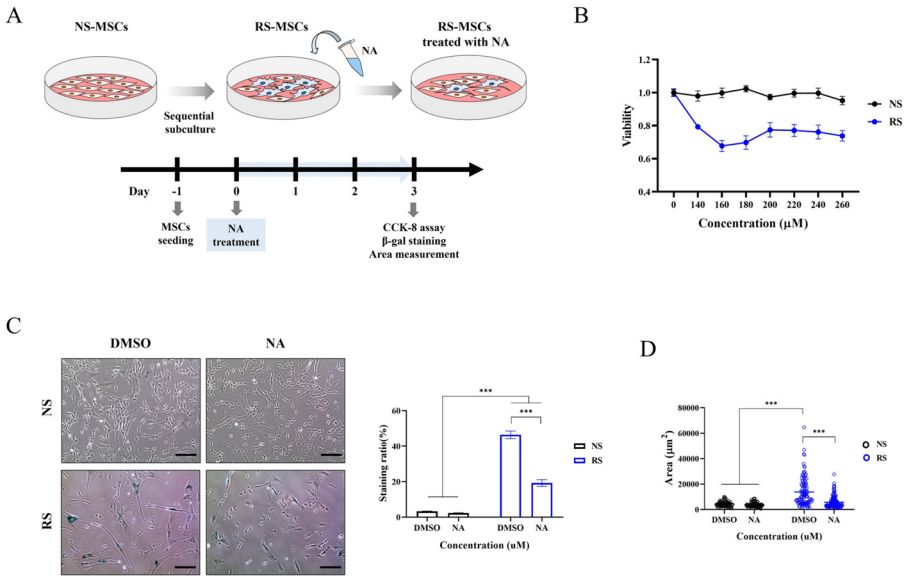

Fig. 2. Nervonic acid (NA) suppressed the replicative senescence of Wharton's jelly-derived mesenchymal stem cells. (A) Experimental scheme for identification of senescence inhibition through NA after induction of replicative senescent mesenchymal stem cells (MSCs). (B) Cell viability was assessed after treatment with various NA concentrations. (C) β-Galactosidase staining (scale bar=250 μm) and (D) area measurement of cells was performed with or without NA. Data are presented as mean±SEM. The significance of the differences was assessed by one-way ANOVA (***$p<0.001$). NS-MSCs: non-senescent MSCs; RS-MSCs: replicative senescent MSCs; CCK-8: Cell Counting Kit-8; DMSO: dimethyl sulfoxide.

fy whether NA inhibits replicative senescence in MSCs derived from various sources. RS-MSCs of AD-MSCs, BM-MSCs, UCB-MSCs, and PL-MSCs were treated with NA for 3 days. The ratio of β-gal-positive cells significantly decreased in all types of human-derived MSCs after NA treatment (Supplementary Fig. S2). Therefore, NA was shown to inhibit senescence in MSCs derived from various sources.

NA reduces the expression of senescence markers in WJ-MSCs

Since NA inhibited the senescence of WJ-MSCs, we determined the expression of senescence markers. The mRNA levels of *p16* and *p21* were highly expressed in RS-MSCs and significantly decreased in NA-treated RS-MSCs (Fig. 3A). The protein levels of p16 and p21 in RS-MSCs were significantly higher than that in NS-MSCs. However, NA significantly decreased p16 expression in RS-MSCs, but did not affect p21 expression (Fig. 3B).

The mRNA expression of SASP markers, one of the characteristics of cellular senescence, was confirmed using qRT-PCR. *IL-6*, *MMP3*, *IGFBP3*, *IGFBP5*, and *IGFBP7* expression was increased by replicative senescence. *MMP3*, *IGFBP3*, *IGFBP5*, and *IGFBP7* decreased significantly in RS-MSCs by NA treatment, while *IL-6* was not affected by NA treatment (Fig. 3C). These results suggested that NA plays an important role in the suppression of replicative senescence.

Effects of NA on stemness, differentiation, and secretion in RS-MSCs

To determine the effect of NA on stemness, FACS was conducted in NS-MSCs and RS-MSCs. MSC-positive markers (CD44, CD73, CD90, CD105, and CD166) and MSC-negative markers (CD14, CD19, CD34, CD45, and HLA-DR [MHC II]) were used. The MSC-positive markers were highly expressed (more than 95%) in NS-MSCs, and their expression marginally decreased in RS-MSCs. NA treatment increased the expression of MSC-positive markers in RS-MSCs, and in particular, the expressions of CD44 and CD73 were significantly increased by NA treatment. However, no significant changes were observed in MSC-negative markers by replicative senescence and NA treatment (Fig. 4A). In RS-MSCs, NA treatment recovered stemness; therefore, osteogenesis and adipogenesis were induced to confirm the effect of NA on differentiation. Replicative senescence interfered with the induction of osteogenesis and adipogenesis in WJ-MSCs. However, NA significantly increased the induction of adipogenesis in RS-MSCs (Fig. 4B).

Single-cell RNA sequencing was performed to identify the difference in gene expression by NA treatment in RS-MSCs. A heat map was used to identify differentially expressed genes, between RS-MSCs and NA-treated RS-

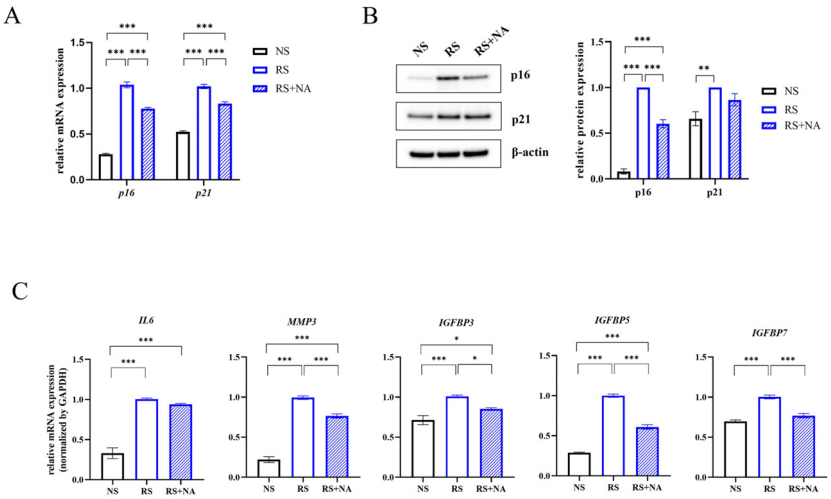

Fig. 3. Nervonic acid (NA) treatment significantly reduced the expression of senescence markers in replicative senescent mesenchymal stem cells (RS-MSCs). (A) mRNA expression of *p16* and *p21*, (B) protein expression of p16 and p21, and (C) mRNA expression of senescence-associated secretory phenotype, including *IL-6, MMP3, IGFBP3, IGFBP5,* and *IGFBP7*, were measured in non-senescent MSCs (NS-MSCs), RS-MSCs, and NA-treated RS-MSCs. Data are presented as mean±SEM. The significance of the differences was assessed by one-way ANOVA (*p<0.05, **p<0.01, ***p<0.001).

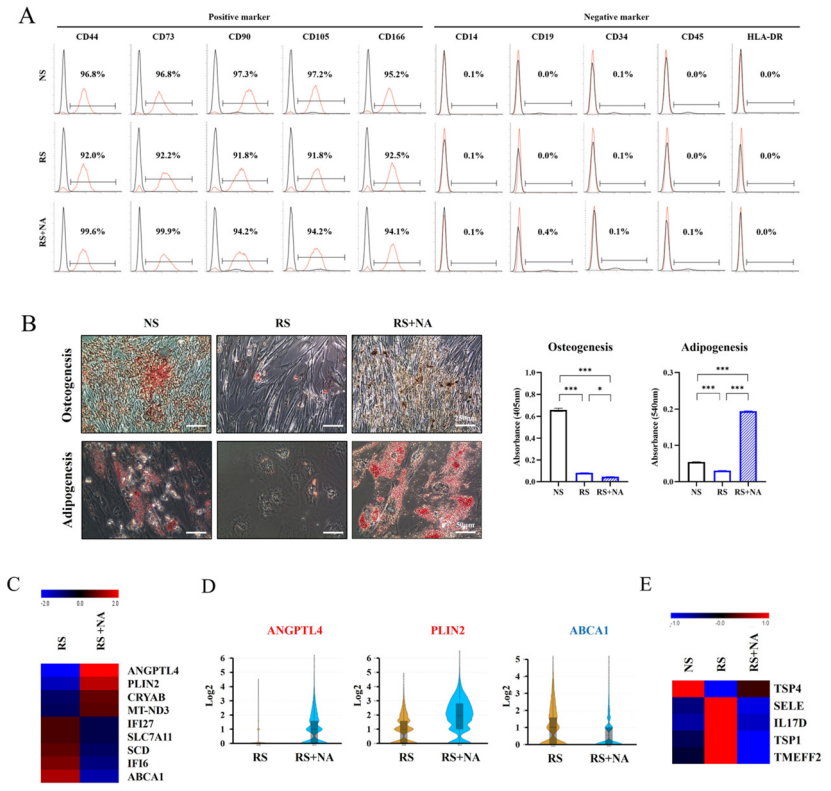

Fig. 4. Effects of nervonic acid (NA) on stemness, differentiation, and secretion in replicative senescent mesenchymal stem cells (RS-MSCs). (A) Expression of cell surface markers determined using flow cytometry analysis. The x-axis depicts fluorescence intensity, and the y-axis depicts cell count. (B) Osteogenesis was confirmed using Alizarin Red S staining (scale bar=250 μm), and adipogenesis was identified using Oil Red O staining (scale bar=50 μm) in non-senescent mesenchymal stem cells (NS-MSCs), RS-MSCs, and NA-treated RS-MSCs. (C) Heat map shows nine differentially expressed genes (fold change>1.5). (D) Violin plot was used to visualize the difference in expression levels and cell number of three genes in RS-MSCs and NA-treated RS-MSCs (fold change>2). (E) The differences in secretory proteins were confirmed using an antibody array. Heat map shows five differentially secreted proteins (fold change>1.5). Data are presented as mean±SEM. The significance of the differences was assessed by one-way ANOVA (*p<0.05, ***p<0.001).

MSCs, with a fold change＞1.5. In the NA-treated RS-MSCs, *ANGPTL4*, *PLIN2*, *CRYAB*, and *MT-ND3* increased and *IFI27*, *SLC7A11*, *SCE*, *IFI6*, and *ABCA1* decreased (Fig. 4C). The violin plot showed that *ANGPTL4*, *PLIN2*, and *ABCA1* were differentially expressed by 2-fold. NA-treated RS-MSCs significantly increased the number of cells with *ANGPTL4* and *PLIN2* expression as well as *ANGPTL4* and *PLIN2* expression. In contrast, in NA-treated RS-MSCs, the expression of *ABCA1* and the number of cells expressing *ABCA1* decreased (Fig. 4D).

To compare the expression of secreted protein between NS-MSCs, RS-MSCs and NA-treated RS-MSCs, an antibody array was conducted. The secretion of E-selectin (SELE), interleukin-17D (IL17D), thrombospondin-1 (TSP1), and transmembrane protein with an EGF-like and two follistatin-like domains 2 (TMEFF2) increased with replicative senescence and decreased with NA treatment. Thrombospondin-4 (TSP4) secretion decreased with replicative senescence and increased with NA treatment (Fig. 4E).

NA-treated NS-MSCs attenuated replicative senescence and increased proliferation

Our results showed that NA is an important metabolite in inhibiting the senescence of RS-MSC. Therefore, we verified whether replicative senescence is delayed by continuous subculture after NA treatment to NS-MSC. NS-MSCs treated with DMSO (0.32%) or NA (160 μM) for 24 hours were cultured sequentially up to passage 10 under the normal culture conditions, and the level of senescence and proliferation of each group were compared (Fig. 5A).

As the subculture progressed, the ratio of β-gal positive cells rapidly increased in DMSO-treated NS-MSCs. However, the rate of β-gal positive cells in NA-treated NS-MSCs was lower than that of DMSO-treated NS-MSCs, at the same passage. At passage 10, the ratio of β-gal positive cells in the DMSO treatment group and the NA treatment group was 24.41% and 9.85%, respectively (Fig. 5B). We also confirmed mRNA expression of aging-related genes at passage 10. *p16* and *p21* expression decreased in the NA treatment group (Fig. 5C). The expression of SASP factors (*IL6*, *MMP3*, *IGFBP3*, *IGFBP5*, and *IGFBP7*) (17) decreased in the NA treatment group (Fig. 5D).

The doubling times of the DMSO treatment group and the NA treatment group were 32.69 and 24.72 hours, respectively (Fig. 5E). NA increases proliferation by attenu-

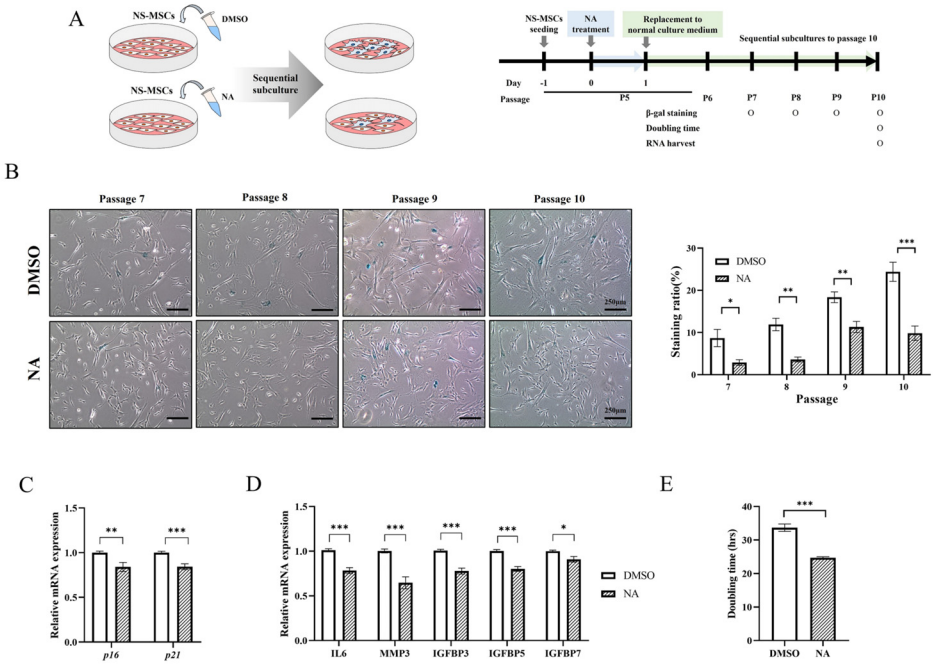

Fig. 5. Nervonic acid (NA)-treated non-senescent mesenchymal stem cells (NS-MSCs) attenuated replicative senescence and increased proliferation in the continuous subculture. (A) Experimental schedule for measuring the effect of NA treatment in NS-MSCs. (B) The analysis of SA-β-galactosidase staining at each passage (scale bar=250 μm). (C) Relative mRNA expression of *p16* and *p21*. (D) Relative mRNA expression of senescence-associated secretory phenotype. (E) Proliferation and doubling time confirmed by Cell Counting Kit-8 assay in NS-MSCs treated with dimethyl sulfoxide (DMSO) or NA at passage 10. Data are presented as mean±SEM and analyzed by two-tailed student's t-test (*p＜0.05, **p＜0.01, ***p＜0.001).

ating replicative senescence and reducing the expression of the senescence marker.

Discussion

MSCs have a high clinical value and are capable of homing to inflammation sites, tissue repair, and differentiation into many cell types. In particular, WJ-MSCs are widely used in cell therapy because of their higher yield and higher expression of pluripotency markers and are an excellent source of non-ethically restrictive MSCs (18). However, cellular senescence weakens therapeutic effect (19) and negatively impacts the use and potential of WJ-MSCs. Therefore, we aimed to suppress cellular senescence in replicative senescent WJ-MSCs.

Cyclin/CDK complex is essential for G1 to S and G2 to M transitions. p16 and p21, cyclin/CDK complex inhibitors, are involved in cell cycle arrest (20). p21 and p16 are highly expressed in early- and late-stage senescence, respectively (21). Chromatin remodeling occurs upon p16 and p21 activation, leading to senescence programs such as SASP production and SA-β-gal activity (22). During replicative senescence, we found that p21 increased significantly in passage 9 and slightly decreased in passage 18, while p16 increased significantly with an increase of β-gal positive cells in passage 18. Therefore, p21 and p16 could determine the early and late senescent states, respectively.

Cellular senescence has been regarded as a permanent cell cycle arrest; however, recent studies have shown that senescent cells can re-enter the cell cycle in certain situations (23). In RS-MSCs, NA did not affect the protein expression of p21, but reduced the protein expression of p16 and the mRNA expression of SASP. It is expected that NA will eliminate RS-MSCs of late senescent state but not the early senescent state. Therefore, the remaining MSCs could re-enter the cell cycle through NA-induced genetic change, thus delaying senescence. Since RS-MSCs of late senescent state were removed by NA, SASP expression was also reduced. Decreased SASP expression contributes to the reduction of SASP secretion and senescence delay. Therefore, NA may be an important metabolite that suppresses senescence.

RS-MSCs reduce stemness and differentiation potential (24). Herein, replicative senescence reduced stemness of WJ-MSCs, but NA reversed this effect by suppressing senescence and significantly increasing CD44 and CD73. CD44 participates in migration, proliferation and invasion (25) and stimulates early angiogenesis in cancers (26). CD73 acts as an anti-inflammatory molecule and promotes cell viability and migration (27). Therefore, NA is likely to improves the therapeutic effects of MSCs by increasing migration and proliferation as well as increasing stemness in RS-MSCs.

In WJ-MSCs, replicative senescence interfered with the induction of differentiation. However, long-term treatment of NA remarkably promoted induction of adipogenesis in RS-MSCs. According to single-cell analysis, NA had a significant effect on lipid metabolism. Fatty acid activates the transcription of angiopoietin-like 4 (*ANGPTL4*) by peroxisome proliferator-activated receptors (28). ANGPTL4 also promotes migration, inhibits apoptosis, and is involved in cancer cell invasion (29, 30). Perilipin 2 is involved in the metabolism of intracellular lipid droplets and age-related diseases (31). ATP-binding cassette transporter A1 regulates cholesterol and phospholipid homeostasis (32). These genes contribute to the stimulation of adipogenesis with long-term NA treatment of RS-MSCs. Therefore, we will conduct further research on the induction of adipogenesis through NA.

MSCs are involved in tissue regeneration by secreting various proteins which promote angiogenesis and inhibit apoptosis (33). TSP4 is involved in blood vessels regeneration and angiogenesis promotion through TGF-β1 in endothelial cells (34). Also, TSP4-overexpressing bone marrow stromal cells increase the proliferation, migration and angiogenesis of human umbilical vein endothelial cells, enhance capillary formation in ischemic boundary zone, and improve therapeutic efficacy by recovering neurological function post-stroke through TGF-β/Smad2/3 signaling pathway (35). TSP1 is upregulated in senescent cells, promoting cell cycle arrest and senescence by increasing p16, p21, and p53. TSP1 participates in angiogenesis, proliferation and cell survival by binding to receptors such as β1 integrin, CD148, CD36, and CD47. CD36 increases with p16, β-galactosidase protein, and SASP in late senescence and suppresses angiogenesis, chemotaxis and cell survival through TSP1 binding. TSP1-CD47 pathway interrupts proliferation, cell cycle progression, angiogenesis and stem cell maintenance, promoting senescence (36). RS-MSCs treated with NA increased TSP4 secretion and decreased TSP1 secretion, which is expected to promote proliferation and angiogenesis, thereby improving the therapeutic effect of MSCs.

Senescent MSCs cause inflammation by producing secretory factors such as cytokines and growth factors, which affect their neighboring cells and accelerate cell aging (37). NA reduces the secretion of inflammatory factors by inhibiting the TLR4/NF-κB pathway in colitis model mice (38). In our study, we found that NA reduced the secretion of inflammatory-related SELE and IL17D in senescent MSCs. SELE

is a pro-inflammatory gene that increases in replicative senescent endothelial cells and is induced by cytokines (39), and IL17D is affiliated to the IL17 family of cytokines involved in inflammation (40). We hypothesize that inflammatory factors were reduced because NA suppressed the expression of cytokines corresponding to SASP. Reduction of inflammatory factors by NA ameliorates senescence, thereby improving the therapeutic efficacy of MSCs.

Under the non-senescent state, WJ-MSCs treated with DMSO had a larger number of β-gal positive cells than WJ-MSCs cultured in normal media. As shown in Supplementary Fig. S3, WJ-MSCs were sensitive to DMSO even at low concentrations. Although 0.32% DMSO did not affect WJ-MSC viability, it induced senescence. Once DMSO provoked senescence in WJ-MSCs, cellular senescence accelerated as the subculture progressed. However, cellular senescence in NA-treated WJ-MSCs was delayed compared to that of DMSO-treated WJ-MSCs, during subsequent repetitive subculture. In addition, as aging was delayed, the expression of aging-related genes decreased, and proliferation increased. Therefore, NA treatment in NS-MSCs attenuates replicative senescence caused by continuous culture. Nevertheless, it is necessary to consider a countermeasure to prevent senescence caused by DMSO since DMSO exposure can promote senescence.

NA regulated cellular senescence through removal of senescent cells at optimal concentration. However, the RS-MSC viability was slightly increased at concentrations higher than the appropriate concentration. This result was observed in all experimental repeats; therefore, it is an NA-associated treatment limitation. This requires further investigation.

We confirmed for the first time that NA inhibits cellular senescence. NA inhibits senescence by removing senescent MSCs and delays further aging by reducing SASP expression. In addition, the NS-MSCs treated with NA are likely to be used as a prolonged treatment because NA attenuates replicative senescence, caused by repetitive subculture and increases proliferative capacity. Therefore, NA is expected to improve the regulation of cellular senescence.

ORCID

Sun Jeong Kim, https://orcid.org/0000-0003-2344-4176
Soojin Kwon, https://orcid.org/0009-0006-1522-7584
Soobeen Chung, https://orcid.org/0009-0008-3464-891X
Eun Joo Lee, https://orcid.org/0009-0003-7371-2121
Sang Eon Park, https://orcid.org/0000-0003-3315-6426
Suk-Joo Choi, https://orcid.org/0000-0002-8946-4789
Soo-Young Oh, https://orcid.org/0000-0003-3002-0048
Gyu Ha Ryu, https://orcid.org/0000-0001-9240-1837
Hong Bae Jeon, https://orcid.org/0000-0003-4420-9968
Jong Wook Chang, https://orcid.org/0000-0001-9335-5510

Funding

This work was supported by the National Research Foundation of Korea (NRF) grant funded by the Korean government (MSIT) (2021R1F1A1064060) and supported by the Korean Fund for Regenerative Medicine funded by the Ministry of Science and ICT, and Ministry of Health and Welfare (RS-2022-00060268). This research was also supported by the Bio & Medical Technology Development Program of the National Research Foundation (NRF) funded by the Ministry of Science & ICT (RS-2023-00223069) and supported by a grant from the Korea Health Technology R&D Project through the Korea Health Industry Development Institute (KHIDI), funded by the Ministry of Health & Welfare, Republic of Korea (grant number: HR22C1363). This work was partly supported by the Collabo R&D between Industry, Academy, and Research Institute of MSS (S3098634), and by Samsung Medical Center (SMO1230051).

Potential Conflict of Interest

There is no potential conflict of interest to declare.

Authors' Contribution

Conceptualization: SJK, SEP. Data curation: SJK, SC. Formal analysis: SJK. Funding acquisition: HBJ, JWC. Investigation: SJK, SK, SC, EJL. Project administration: SJK, SK, SC. Resources: SJC, SYO, GHR. Software: SJK. Supervision: HBJ, JWC. Validation: SK, SC. Visualization: SJK, SK. Writing – original draft: SJK, SK, SC. Writing – review and editing: HBJ, JWC.

Supplementary Materials

Supplementary data including three figures can be found with this article online at https://doi.org/10.15283/ijsc23101

References

1. Hernandez-Segura A, Nehme J, Demaria M. Hallmarks of cellular senescence. Trends Cell Biol 2018;28:436-453.
2. Kim SJ, Park SE, Jeong JB, et al. Wharton's jelly-derived mesenchymal stem cells with high aurora kinase A expression show improved proliferation, migration, and therapeutic potential. Stem Cells Int 2022;2022:4711499.
3. Weng Z, Wang Y, Ouchi T, et al. Mesenchymal stem/stromal cell senescence: hallmarks, mechanisms, and combating strategies. Stem Cells Transl Med 2022;11:356-371.

4. Zhou X, Hong Y, Zhang H, Li X. Mesenchymal stem cell senescence and rejuvenation: current status and challenges. Front Cell Dev Biol 2020;8:364.
5. Liu J, Ding Y, Liu Z, Liang X. Senescence in mesenchymal stem cells: functional alterations, molecular mechanisms, and rejuvenation strategies. Front Cell Dev Biol 2020;8:258.
6. Sharma R. Emerging interrelationship between the gut microbiome and cellular senescence in the context of aging and disease: perspectives and therapeutic opportunities. Probiotics Antimicrob Proteins 2022;14:648-663.
7. Parker A, Romano S, Ansorge R, et al. Fecal microbiota transfer between young and aged mice reverses hallmarks of the aging gut, eye, and brain. Microbiome 2022;10:68.
8. Zheng W, Kollmeyer J, Symolon H, et al. Ceramides and other bioactive sphingolipid backbones in health and disease: lipidomic analysis, metabolism and roles in membrane structure, dynamics, signaling and autophagy. Biochim Biophys Acta 2006;1758:1864-1884.
9. Li Q, Chen J, Yu X, Gao JM. A mini review of nervonic acid: source, production, and biological functions. Food Chem 2019;301:125286.
10. Yu J, Yuan T, Zhang X, Jin Q, Wei W, Wang X. Quantification of nervonic acid in human milk in the first 30 days of lactation: influence of lactation stages and comparison with infant formulae. Nutrients 2019;11:1892.
11. Wu R, Zhong S, Ni M, et al. Effects of *Malania oleifera Chun* oil on the improvement of learning and memory function in mice. Evid Based Complement Alternat Med 2020; 2020:8617143.
12. Kwon S, Ki SM, Park SE, et al. Anti-apoptotic effects of human Wharton's jelly-derived mesenchymal stem cells on skeletal muscle cells mediated via secretion of XCL1. Mol Ther 2016;24:1550-1560.
13. Palumbo P, Lombardi F, Siragusa G, Cifone MG, Cinque B, Giuliani M. Methods of isolation, characterization and expansion of human adipose-derived stem cells (ASCs): an overview. Int J Mol Sci 2018;19:1897.
14. Choi YS, Park YB, Ha CW, et al. Different characteristics of mesenchymal stem cells isolated from different layers of full term placenta. PLoS One 2017;12:e0172642.
15. Kim JY, Kim DH, Kim DS, et al. Galectin-3 secreted by human umbilical cord blood-derived mesenchymal stem cells reduces amyloid-beta42 neurotoxicity *in vitro*. FEBS Lett 2010;584:3601-3608.
16. Dominici M, Le Blanc K, Mueller I, et al. Minimal criteria for defining multipotent mesenchymal stromal cells. The International Society for Cellular Therapy position statement. Cytotherapy 2006;8:315-317.
17. Byun HO, Lee YK, Kim JM, Yoon G. From cell senescence to age-related diseases: differential mechanisms of action of senescence-associated secretory phenotypes. BMB Rep 2015; 48:549-558. Erratum in: BMB Rep 2016;49:641-650.
18. Kamal MM, Kassem DH. Therapeutic potential of Wharton's jelly mesenchymal stem cells for diabetes: achievements and challenges. Front Cell Dev Biol 2020;8:16.
19. Neri S, Borzì RM. Molecular mechanisms contributing to mesenchymal stromal cell aging. Biomolecules 2020;10:340.
20. Li J, Han S, Cousin W, Conboy IM. Age-specific functional epigenetic changes in p21 and p16 in injury-activated satellite cells. Stem Cells 2015;33:951-961.
21. Stein GH, Drullinger LF, Soulard A, Dulić V. Differential roles for cyclin-dependent kinase inhibitors p21 and p16 in the mechanisms of senescence and differentiation in human fibroblasts. Mol Cell Biol 1999;19:2109-2117.
22. Liao Z, Yeo HL, Wong SW, Zhao Y. Cellular senescence: mechanisms and therapeutic potential. Biomedicines 2021; 9:1769.
23. Kumari R, Jat P. Mechanisms of cellular senescence: cell cycle arrest and senescence associated secretory phenotype. Front Cell Dev Biol 2021;9:645593.
24. Chinnadurai R, Rajan D, Ng S, et al. Immune dysfunctionality of replicative senescent mesenchymal stromal cells is corrected by IFNγ priming. Blood Adv 2017;1:628-643.
25. Nam K, Oh S, Lee KM, Yoo SA, Shin I. CD44 regulates cell proliferation, migration, and invasion via modulation of c-Src transcription in human breast cancer cells. Cell Signal 2015;27:1882-1894.
26. Ludwig N, Szczepanski MJ, Gluszko A, et al. CD44(+) tumor cells promote early angiogenesis in head and neck squamous cell carcinoma. Cancer Lett 2019;467:85-95.
27. Petruk N, Tuominen S, Åkerfelt M, et al. CD73 facilitates EMT progression and promotes lung metastases in triple-negative breast cancer. Sci Rep 2021;11:6035.
28. Dijk W, Kersten S. Regulation of lipoprotein lipase by Angptl4. Trends Endocrinol Metab 2014;25:146-155.
29. Adhikary T, Brandt DT, Kaddatz K, et al. Inverse PPARβ/δ agonists suppress oncogenic signaling to the ANGPTL4 gene and inhibit cancer cell invasion. Oncogene 2013;32: 5241-5252.
30. Li X, Chen T, Shi Q, et al. Angiopoietin-like 4 enhances metastasis and inhibits apoptosis via inducing bone morphogenetic protein 7 in colorectal cancer cells. Biochem Biophys Res Commun 2015;467:128-134.
31. Conte M, Franceschi C, Sandri M, Salvioli S. Perilipin 2 and age-related metabolic diseases: a new perspective. Trends Endocrinol Metab 2016;27:893-903.
32. Attie AD, Kastelein JP, Hayden MR. Pivotal role of ABCA1 in reverse cholesterol transport influencing HDL levels and susceptibility to atherosclerosis. J Lipid Res 2001;42:1717-1726.
33. Tao H, Han Z, Han ZC, Li Z. Proangiogenic features of mesenchymal stem cells and their therapeutic applications. Stem Cells Int 2016;2016:1314709.
34. Muppala S, Xiao R, Krukovets I, et al. Thrombospondin-4 mediates TGF-β-induced angiogenesis. Oncogene 2017;36: 5189-5198.
35. Zhang Q, Zhou M, Wu X, et al. Promoting therapeutic angiogenesis of focal cerebral ischemia using thrombospondin-4 (TSP4) gene-modified bone marrow stromal cells (BMSCs) in a rat model. J Transl Med 2019;17:111.
36. Isenberg JS, Roberts DD. Thrombospondin-1 in maladaptive aging responses: a concept whose time has come. Am J Physiol Cell Physiol 2020;319:C45-C63.

37. Liu Y, Chen Q. Senescent mesenchymal stem cells: disease mechanism and treatment strategy. Curr Mol Biol Rep 2020;6:173-182.
38. Yuan SN, Wang MX, Han JL, et al. Improved colonic inflammation by nervonic acid via inhibition of NF-κB signaling pathway of DSS-induced colitis mice. Phytomedicine 2023;112:154702.
39. Ito TK, Yokoyama M, Yoshida Y, et al. A crucial role for CDC42 in senescence-associated inflammation and atherosclerosis. PLoS One 2014;9:e102186.
40. Lee Y, Clinton J, Yao C, Chang SH. Interleukin-17D promotes pathogenicity during infection by suppressing CD8 T cell activity. Front Immunol 2019;10:1172.